Author Manuscript

Author Manuscript

Author Manuscript

Author Manuscript

HHS Public Access

Author manuscript

Oncogene. Author manuscript; available in PMC 2019 June 20.

Published in final edited form as:

Oncogene. 2019 April ; 38(16): 2984–2993. doi:10.1038/s41388-018-0636-y.

Targeting the α4-α5 dimerization interface of K-RAS inhibits tumor formation *in vivo*

Imran Khan[#1,2,3,4], **Russell Spencer-Smith**[#1,2], and **John P. O'Bryan**[1,2,3,4,+]

[1]Department of Pharmacology, University of Illinois Cancer Center, University of Illinois at Chicago, Chicago, IL 60612

[2]Department of Cell, Jesse Brown VA Medical Center, Chicago

[3]Molecular Pharmacology and Experimental Therapeutics, Hollings Cancer Center, Medical University of South Carolina, Charleston, SC 29425

[4]Ralph H. Johnson VA Medical Center, Charleston, SC 29401

[#] These authors contributed equally to this work.

Abstract

RAS genes are the most commonly mutated oncogenes in human cancers. Despite tremendous efforts over the past several decades, however, RAS-specific inhibitors remain elusive. Thus, targeting RAS remains a highly sought after goal of cancer research. Previously, we reported a new approach to inhibit RAS-dependent signaling and transformation *in vitro* through targeting the α4-α5 dimerization interface with a novel RAS-specific monobody, termed NS1. Expression of NS1 inhibits oncogenic K-RAS and H-RAS signaling and transformation *in vitro*. Here, we evaluated the efficacy of targeting RAS dimerization as an approach to inhibit tumor formation *in vivo*. Using a doxycycline (DOX) regulated NS1 expression system, we demonstrate that DOX-induced NS1 inhibited oncogenic K-RAS driven tumor growth *in vivo*. Furthermore, we observed context-specific effects of NS1 on RAS-mediated signaling in 2D vs 3D growth conditions. Finally, our results highlight the potential therapeutic efficacy of targeting the α4-α5 dimerization interface as an approach to inhibit RAS-driven tumors *in vivo*.

Keywords

RAS GTPases; monobody; tumorigenesis; oncogenesis

Users may view, print, copy, and download text and data-mine the content in such documents, for the purposes of academic research, subject always to the full Conditions of use:http://www.nature.com/authors/editorial_policies/license.html#terms

[+]Address correspondence to: John P. O'Bryan, Department of Cell and Molecular Pharmacology and Experimental Therapeutics, Hollings Cancer Center, Medical University of South Carolina, 86 Jonathan Lucas St. MSC 955, Rm HO712E, Charleston, SC 29412; Tel: 843-792-8343; Fax: 843-792-3200, obryanjo@musc.edu.

Competing interests: The authors declare that they have no competing interests.

Author Manuscript Author Manuscript Author Manuscript Author Manuscript

Introduction

RAS proteins are binary molecular switches that cycle between an inactive, GDP-bound state and an active, GTP-bound state(1). Normally, RAS regulates a variety of physiological processes including growth, proliferation, survival and motility(2,3). Following growth factor stimulation of cells, guanine nucleotide exchange-factors (GEFs) promote the release of GDP from RAS resulting in the subsequent binding of GTP and engagement of effector proteins. Activated RAS-GTP is converted back to its inactive GDP-bound state through the intrinsic GTPase activity of the protein, which is enhanced by GTPase-accelerating proteins (GAPs)(4–6). However, oncogenic activation of RAS occurs through point mutations at various hotspots, predominantly codons 12, 13, and 61. These mutations impair the intrinsic GTPase activity of RAS and interfere with GAP-binding thereby resulting in constitutive engagement of effector pathways(7). Mutations in one of three RAS genes (*H-RAS, K-RAS* and *N-RAS*) occur in nearly 30% of human tumors, with *K-RAS* mutations accounting for nearly 85% of these mutants(1,7). The importance of RAS in cancer is supported by numerous lines of evidence demonstrating the role of mutant RAS in driving tumor development as well as the dependence of RAS mutant tumors on the continued presence of oncogenic RAS for tumor maintenance. Thus, much effort has been devoted to the development of therapeutic approaches to inhibit RAS *in vivo*.

Despite the success of ATP-competitive inhibitors at blocking kinases, targeting guanine nucleotide binding by RAS proteins has been largely unsuccessful due in part to the picomolar affinity of RAS for GTP/GDP. Subsequent efforts have focused on interfering with the membrane localization of RAS, which is required for its biological activity. Farnesyltransferases (FTases) mediate the posttranslational attachment of farnesyl lipids to the C-terminal CaaX motif, which is essential for membrane association of RAS. Although farnesyltransferase inhibitors (FTIs) showed significant efficacy in reducing growth of H-RAS driven tumors in preclinical studies, these inhibitors have been ineffective clinically due to the fact that most RAS-mutant solid tumors possess either K-RAS or N-RAS mutations. Unlike H-RAS, these RAS proteins evade the inhibitory effect of FTIs due to alternative lipidation mechanisms(8,9). Therefore, new therapeutic approaches to inhibit RAS are needed.

Accumulating evidence reveals a previously underappreciated aspect of RAS biology, namely formation of RAS dimers and higher order nanoclusters(10–13). Despite the inability of RAS to form dimers in solution or on artificial membrane structures(14,15), significant evidence points to a role for RAS dimerization in the activation of downstream pathways(16). The lack of RAS dimerization *in vitro* versus in cells may stem from the involvement of additional cellular factors that assist in dimerization of RAS at the plasma membrane. However, the lack of an available means to specifically disrupt these RAS dimers/nanoclusters has prevented analysis of their importance in RAS signaling.

We isolated a high-affinity synthetic binding protein (monobody) called NS1 that selectively binds H-RAS and K-RAS with high affinity(17). Biochemical and structural analyses revealed that NS1 binds the α4-α5 interface of RAS, disrupting RAS dimerization and nanoclustering(17,18). NS1 potently inhibited oncogenic RAS-mediated RAF dimerization

Author Manuscript Author Manuscript Author Manuscript Author Manuscript

and activation revealing for the first time the importance of RAS self-association through the α4-α5 interface as a requisite step in the activation of downstream effectors such as RAF(17). While expression of NS1 in cells potently inhibited H/K-RAS-mediated signaling and transformation *in vitro*, the question remains whether targeting the α4-α5 interface represents a viable approach to inhibit oncogenic RAS *in vivo*. Here, we evaluated the efficacy of using a chemically regulated, genetically encoded NS1 construct to interfere with RAS dimerization/nanoclustering as a means of inhibiting RAS-driven tumor development *in vivo*. Our findings indicate that targeting the α4-α5 interface represents a potential approach to block RAS-driven tumors *in vivo*.

Results:

Inducible expression of NS1 selectively inhibits signaling and proliferation of K-RAS-mutant human tumor cells.

To determine whether targeting the α4-α5 interface was sufficient to block RAS-driven tumor formation *in vivo*, we established a DOX-regulated expression system to generate NS1 inducible subclones of various human tumor cell lines harboring mutations in either *KRAS* or *NRAS*. Our prior results demonstrated the specificity of NS1 at binding and inhibiting K-RAS and H-RAS *in vitro* but not N-RAS due to sequence-specific differences in these RAS isoforms(17). Thus, we anticipated that NS1 would inhibit K-RAS but not N-RAS mutant human tumor lines. We isolated stable subclones of CFPAC-1 pancreatic cancer cells [K-RAS(G12V) mutant], HEC1A endometrial cancer cells [K-RAS(G12D) mutant], H1792 lung adenocarcinoma cells [K-RAS(G12C) mutant] and H1299 non-small cell lung carcinoma cells [N-RAS(Q61K)] mutant. The effects of NS1 expression on RAS signaling varied between tumor lines (Fig 1). DOX-induced CFP-NS1 expression decreased pERK levels in both CFPAC-1 and H1792 lines (Fig. 1A and Supplementary Figure 1B). In addition, transient expression of CFP-NS1 reduced pERK levels in PANC-1 pancreatic cancer cells [K-RAS(G12D) mutant], and H1915 non-small cell lung carcinoma cells [H-RAS(Q61L) mutant] (Supplementary Figure 3A and B). However, there was no change in pERK levels in HEC1A (Fig. 1B) consistent with prior studies demonstrating that deletion of mutant K-RAS attenuated the tumorigenic properties of HEC1A independent of effects on the Raf/MEK/ERK pathway (19,20). As anticipated, NS1 did not affect ERK activation in H1299 cells [N-RAS(Q61K) mutant] or SK-N-AS neuroblastoma cells [N-RAS(Q61K) mutant] demonstrating that the isotype specificity of NS1 is maintained in tumor cells (Fig. 1C and Supplementary Figure 3C). In contrast to the effects on pERK, NS1 expression increased pAKT levels in CFPAC-1, H1792, and HEC1A cells (Fig. 1A, B and Supplementary Figure 1C). While the effects of NS1 on RAS signaling were cell type dependent, NS1 expression reduced the proliferation of K-RAS mutant, but not N-RAS mutant, tumor cells (Fig. 1D–F and Supplementary Figures 1C and D).

To further validate that the effects of NS1 were mediated specifically by NS1, we generated DOX-inducible, CFP-expressing versions of various mutant K-RAS mutant cells. Selective expression of CFP was observed in all lines by DOX induction; however, DOX induction of CFP did not affect RAS signaling (Supplementary Figure 4). These results demonstrate that

Author Manuscript Author Manuscript Author Manuscript Author Manuscript

the inhibition of ERK is due specifically to NS1 expression and not CFP or non-specific effects of DOX.

Targeting the RAS α4-α5 interface inhibits anchorage-independent growth of K-RAS mutant tumor cells

Next, we evaluated the ability of NS1 to inhibit the growth of tumor cells in 3D. Consistent with the effects of NS1 on RAS-mediated cell proliferation in 2D culture, NS1 inhibited the anchorage-independent growth of K-RAS mutant tumor lines (CFPAC-1 and HEC1A) in soft agar but did not affect the growth of N-RAS-mutant cells (H1299) (Fig. 2). Similar results were observed with various HEC1A derived isogenic cell lines (Supplementary Figure 2). These results demonstrate the efficacy of NS1 at specifically inhibiting the 3D growth of K-RAS but not N-RAS mutant tumor cells.

Inhibiting RAS dimerization blocks the growth of K-RAS-driven tumors *in vivo*.

Given the ability of NS1 to inhibit the *in vitro* growth of K-RAS mutant cells in both 2D and 3D, we next assessed the efficacy of targeting the α4-α5 interface as an approach to inhibit RAS-driven tumorigenesis *in vivo*. RAS mutant tumor cells stably transfected with DOX-inducible NS1 were injected subcutaneously (s.c.) into athymic nude mice. Two days following injection, mice were randomly segregated into DOX treated (+DOX) or untreated groups (-DOX). DOX-induced expression of NS1 significantly inhibited the growth of both CFPAC-1 and HEC1A tumors but did not affect the growth of N-RAS-mutant H1299 tumors (Figs. 3A&B and 4). Analysis of tumor lysates revealed that NS1 was expressed in all DOX-treated groups, but attenuated ERK activation only in K-RAS mutant tumors (CFPAC-1 and HEC1A) and not N-RAS mutant tumors (H1299) (Fig. 3C, D and Fig. 5).

Next, we evaluated the efficacy of NS1 at reducing tumor burden in established tumors. CFPAC-1 or HEC1A cells were injected s.c. into athymic nude mice. Once tumors attained an average size of 50–70 mm^3 (Day 9), mice were randomized and divided into no DOX (-DOX) and DOX treated (+DOX Day 9) cohorts. NS1 induction slowed tumor progression in DOX-treated mice and this effect was more pronounced in HEC1A versus CFPAC-1 cells (Fig. 4).

RAS inhibition results in context-dependent effects on signaling pathways

When expressed in HEC1A cells grown on tissue culture dishes, NS1 decreased proliferation without affecting ERK-MAPK activation (Figs. 1B, E and 2B). In contrast, NS1 reduced both proliferation and ERK activation in CFPAC-1 cells grown under similar conditions (Figs. 1A, D and 2A). However, analysis of tumors derived from HEC1A and CFPAC-1 cells revealed that NS1 decreased pERK levels in both lines (Figs. 3C and5). Western blot analysis of tumor lysates confirmed the selective expression of NS1 in tumors from DOX-treated mice for both CFPAC-1 and HEC1A tumors. In contrast to the results with HEC1A cells grown in 2D conditions, NS1 expression at both initial and later time points of tumor growth resulted in decreased pERK levels in tumors. However, the effects of NS1 on AKT activation were less dramatic than effects on ERK, with only a slight decrease in pAKT levels upon induction of NS1 expression at either time point (Fig. 5A). For CFPAC-1 derived tumors, the effects of NS1 on ERK-MAPK signaling arm were consistent

Author Manuscript Author Manuscript Author Manuscript Author Manuscript

with cell culture data. However, the effects on PI3K-AKT signaling in 3D differed. While NS1 appeared to augment AKT activity under 2D growth conditions, we observed a significant decrease in pAKT levels in CFPAC1 tumors *in vivo* upon NS1 induction (compare Figs. 1A and 5B).

Inhibiting RAS dimerization induces caspase-3 activation and apoptosis in K-RAS mutant tumors

Next, we examined whether inhibition of RAS dimerization altered the survival of tumor cells *in vivo*. Caspase-3 was used as an indicator of apoptosis induction since different upstream pathways leading to apoptosis depend on caspase-3 induction for final apoptotic execution(21). NS1 induction resulted in activation of caspase-3 in K-RAS mutant (CFPAC-1 and HEC1A) but not N-RAS mutant (H1299) tumors (Fig. 6). Surprisingly, the level of caspase-3 activation was higher in tumors treated with DOX at later times (compared Day 2 vs Day 9 treatment cohorts) for both HEC1A and CFPAC-1 derived tumors (Fig. 6).

Discussion

Given the prominence of activating RAS mutations in human cancers and the importance of mutant RAS as a driver of tumorigenesis, there has been a great deal of interest in therapeutically targeting RAS(1,7). Although initial efforts to therapeutically inhibit RAS by blocking the C-terminal farnesylation of the protein have been disappointing, recent results with mutation-specific inhibitors have provided significant hope for the possibility of pharmacologically inhibiting RAS(22). Shokat and colleagues utilized a novel tethering approach to selectively target the thiol group of RAS(G12C) mutant resulting in the isolation of several inhibitor compounds that lock RAS into the GDP-bound conformation while also disrupting RAS interaction with Sos. Thus, these compounds result in accumulation of RAS in the inactive, GDP-bound state. Subsequent improvements to the chemistry of these lead compounds have resulted in the most recent interation, ARS-1620, which demonstrates selective inhibition of K-RAS(G12C) mutant tumor models *in vivo*(23). While these results provide significant hope for development of an effective RAS therapeutic, such compounds will be limited to treating G12C mutant tumors. Thus, identification of more broadly efficacious inhibitors that target mutant RAS proteins remains an unmet need.

Selective expression of NS1 decreased proliferation of K-RAS but not N-RAS driven tumor cells consistent with our prior analysis of NS1 specificity. These effects were corroborated by the potency of NS1 in abrogating anchorage-independent growth of K-RAS, but not N-RAS, mutant tumor cells in soft agar assays. However, the impact of NS1 on RAS signaling in 2D-adherent tissue culture conditions was varied. NS1 decreased ERK activity in CFPAC-1 pancreatic and H1792 lung cancer cells each of which harbors a mutant K-RAS allele (G12V and G12C, respectively) further demonstrating the importance of the α4-α5 dimerization in oncogenic RAS signaling. In contrast, NS1 did not affect ERK activity in the HEC1A cells grown in culture despite the presence of oncogenic K-RAS(G12D) mutant. Similar results were obtained with isogenic derivatives of HEC1A cells in which either the WT or mutant K-RAS allele was deleted. These results are consistent with previous

Author Manuscript Author Manuscript Author Manuscript Author Manuscript

reports(19,20) demonstrating that ERK activity in HEC1A cells is unaffected by deletion (or inhibition) of K-RAS, at least under 2D growth conditions.

The effects of NS1 on K-RAS signaling, however, were highly dependent upon context. Under 2D-adherent culture conditions, NS1 increased AKT activity in K-RAS mutant tumor lines (HEC1A, CFPAC-1 and H1792) despite inhibiting ERK activation in CFPAC1 and H1792 cells and reducing the growth of all three lines in culture. A paradoxical observation of elevated pAKT levels on loss of K-RAS has been recently reported by others(24). These results were initially surprising given our previous findings that NS1 expression reduced activation of ERK and AKT by both oncogenic H-RAS and K-RAS when transiently co-expressed in cells(17). Furthermore, NS1 expression in HEC1A cells did not affect ERK activation *in vitro* despite significantly inhibiting the proliferation of these cells. However, when cells were grown under 3D conditions, different results were observed. NS1 expression in HEC1A tumors reduced pERK levels regardless of whether NS1 was induced at the time of cell inoculation or once tumors formed. Other groups have reported context dependent effects of K-RAS inhibition as well. Vartanian et al observed varied dependence on mutant K-RAS in cells grown in culture vs anchorage-independent conditions, with cells exhibiting the strongest dependence on mutant K-RAS under the later conditions(20). Treatment of K-RAS(G12C) mutant cells with ARS-1620 resulted in consistent growth inhibition of cells grown as spheroids but had more varied effects on cells grown under 2D-adherent conditions(23). Despite these varied effects on signaling under different conditions, targeting the α4-α5 dimerization interface nonetheless inhibited growth of K-RAS mutant tumor cells *in vivo*. Further, targeting the α4-α5 interface of RAS induced apoptosis in K-RAS but not N-RAS mutant tumors. The ability of NS1 to inhibit K-RAS but not N-RAS mutant tumors further illustrates the specificity of NS1 and the lack of “off-target” effects.

While targeting the α4-α5 dimerization interface with NS1 inhibits establishment of K-RAS mutant tumors, inhibiting RAS dimerization may also be efficacious at reducing tumor growth once tumors are established. Expression of NS1 reduced HEC1A tumor progression *in vivo*. However, established CFPAC-1 tumors appeared more refractory to the inhibitory effects of NS1. The lack of tumor regression may stem from incomplete or insufficient NS1 expression in a subpopulation of cells within the tumor. Alternatively, it is possible that a subpopulation of tumor cells has become resistant to the inhibitory effects of NS1 resulting in the outgrowth of a resistant population. Indeed, analysis of cell lines derived from individual tumors expressing NS1 suggests that some tumors may have developed a resistance to the effects of NS1 (unpublished observations). Defining the mechanism of such resistance may reveal alternative mechanisms through which tumor cells can adapt to RAS inhibition and thus affect the therapeutic efficacy of RAS inhibitors in the clinic.

The importance of the α4-α5 interface in K-RAS tumorigenesis is further supported by the recent work of Ambrogio et al (25). They demonstrate that mutations in the α4-α5 region that disrupt dimerization reduce the oncogenic activity of K-RAS. Interestingly, such dimerization-disrupting mutations reduced ERK activation in tumors but not in 2D-adherent culture conditions further supporting the growing evidence that RAS signaling is context dependent(25). In addition, the ability of wild-type K-RAS to heterodimerize with mutant K-RAS through this interface contributed to the sensitivity of lung tumor cells to MEK

Author Manuscript Author Manuscript Author Manuscript Author Manuscript

inhibitors and also provided a mechanistic explanation for the ability of the wild type allele to inhibit the oncogenic version(25). Thus, targeting this region with small molecules may provide a novel approach to inhibit K-RAS directly while also sensitizing K-RAS mutant cells to inhibitors of downstream signaling pathways.

Our results indicate that targeting the α4-α5 dimerization interface of K-RAS represents a valid approach to therapeutically inhibit K-RAS driven tumors *in vivo*. Although NS1 in its current form is not a viable therapeutic given its large size and inability to penetrate cells, our work nevertheless demonstrates the "drug-like" activity of a genetically encoded NS1. These findings provide support to the goal of developing small molecule mimetics of NS1 that directly bind the α4-α5 interface. Such molecules may provide an opportunity to therapeutically inhibit RAS through disrupting RAS dimerization/nanoclustering, although such an approach may not provide selectivity in targeting mutationally activated vs wild type RAS(16,17). Interestingly, we have observed that NS1 inhibits K-RAS mutant cells without affecting the proliferation of fibroblasts (HEK293 or NIH/3T3) grown in culture (Khan, I. and O'Bryan, J.P., unpublished observations). This lack of "off-target" toxicity may stem from the selectivity of NS1 for H/K-RAS allowing for residual N-RAS function to drive proliferation in these NS1-expressing cells. Thus, it would be critical that such small molecules, like NS1, maintain isoform selectivity given that loss of RAS in most adult tissues is not compatible with life (6). Alternatively, the level of NS1 may be sufficient to inhibit oncogenic RAS without completely ablating wild type RAS activity. In this instance, dosing of an NS1 mimetic would be critical in achieving the necessary therapeutic index.

Although it is unclear from our studies whether targeting α4-α5 dimerization interface will lead to tumor regression, it is nevertheless clear that inhibiting K-RAS dimerization reduces overall tumor burden. Thus, combining dimerization inhibitors with inhibitors of RAS effector pathways such as MEK or mTOR, may provide a more effective strategy for treating K-RAS mutant cancers.

Materials and Methods

Cell culture

All cell lines were cultured as recommended by ATCC and were authenticated by short-tandem repeat (STR) profiling performed by the Research Resource Center at UIC. CFPAC-1, pancreatic cancer origin with endogenous K-RAS(G12V) mutation were provided by Dr. Andrei Karginov; PANC-1 having K-RAS(G12D) mutation was obtained from Dr. Gregory Thatcher; HEC1A endometrial cancer line having K-RAS(G12D) mutation obtained from Dr. Todd Waldman; lung carcinoma lines H1792 with K-RAS(G12C) mutation and H1299 with N-RAS(Q61K) mutation were provided by Dr. Robert Winn; H1915 lung carcinoma cells with HRAS(Q61L) mutation was obtained from ATCC; SK-N-AS neuroblastoma line with N-RAS(Q61K) mutation was obtained from Dr. Bernard Weisman. DOX-inducible NS1 expressing cell lines were generated by lentiviral infection of cells using the pTRIPz-CFP-NS1 construct as previously described(17). Infected cells were selected in puromycin and resistant colonies pooled to generate polyclonal lines that were used for all subsequent analyses.

Author Manuscript Author Manuscript Author Manuscript Author Manuscript

Immunoblotting

Cell lysates were prepared using PLC cell lysis buffer (50 mM HEPES, pH 7.5, 150 mM NaCl, 10% glycerol, 1% Triton X-100, 1 mM EGTA, 1.5 mM magnesium chloride, 100 mM sodium fluoride supplemented with 1 mM vanadate, 10μg/ml leupeptin and 10μg/ml aprotinin). The following antibodies were used: α-ERK1/2, 1:2,000 dilution (9102L), α-phospho-ERK1/2, 1:2,000 dilution (9101L), α-AKT, 1:4,000 dilution (9272S), α-phospho-AKT (S473), 1:1,000 dilution (9271S) and α-phospho-AKT (T308), 1:1,000 dilution (9275S), all purchased from Cell Signaling Technology. Monoclonal α-FLAG-M2 antibody, 1:4,000 dilution (F3165–1MG) and α-FLAG polyclonal antibody, 1:2,000 dilution (F7425-. 2MG), α-β-actin, 1:10000 dilution (A2066) were purchased from Sigma-Aldrich. α-Caspase-3 1: 1,000 (sc-56053) and α-Vinculin 1: 3,000 dilution (sc-73614) were purchased from Santa Cruz Biotechnology.

Cell viability assays

CFPAC-1, HEC1A and H1299 cells (1,000 per well) were plated on 24-well plates in complete medium (DMEM with 10% FBS plus 1μg/ml puromycin and 2μg/ml doxycycline to induce expression from the pTRIPz construct) for the indicated number of days. On the indicated day, medium was removed and replaced with 100μl of serum-free DMEM, cells were harvested after 30 min at 37°C. Viability was assayed using Cell Titer Glow (Promega). Luminescence was quantified on a Dynex 96-well microtiter plate luminometer according to the manufacturer's instructions. Results are presented as the average +/− *s.d.* of two experiments each performed with triplicate wells.

Soft agar colony formation

Assays were performed essentially as described(26). A base agar layer (0.5% agar) was prepared by mixing 1 part of 5% stock agar with 9 parts media. Two ml's of this base agar was then added to each well of a 6-well tissue culture plate and allowed to solidify at room temperature. Cells were trypsinized and counted, then diluted to 5000 cells per well for final agar concentration of 0.33% (1ml media + 2ml of 0.5% agar). Agar/cell suspension mixture was then pipetted on top of the base agar layer, and allowed to set at RT. The plates were placed in a 37°C / 5% CO_2 incubator overnight, cells were fed 1–2x per week by careful drop wise addition of growth media to top layer. Two μg/ml doxycycline (DOX) was added to experimental wells to induce expression of NS1. Three weeks after platting cells were stained using MTT; 100μl of 2mg/ml solution of MTT was used for each well. Colony number and average colony size were quantified using ImageJ. Results represent the average colony number per well from 3 wells ± *s.d.*.

Xenograft tumor assays

Six weeks old male or female athymic nude mice from Charles River Laboratories (CRL) were housed in filter-topped cages and received food and water *ad libitum*. Animal experiments were approved by the Institutional Animal Care and Use committees at all institutions. Power analysis performed prior to initiation of animal experiments indicated that three mice per group would detect a 50% reduction in tumor volume (assume 1.8 cm^3 +/− 0.9 cm^3 *s.d.* and 0.9 cm^3 +/− 0.4 cm^3 *s.d.*) with 95% confidence using statistical power

Author Manuscript Author Manuscript Author Manuscript Author Manuscript

calculators at https://www.dssresearch.com/KnowledgeCenter/toolkitcalculators/samplesizecalculators.aspx. Tumors were generated by subcutaneous injection into the right lower flank with 10×10^6 CFPAC-1 or H1299 cells; 5×10^6 HEC1A cells suspended in 60μl of media and 60μl matrigel (1:1 ratio). Twelve mice were used for each cell type. However, one mouse was excluded from the CFPAC-1 -DOX group and one mouse from the H1299 +DOX group due to lack of tumor development likely stemming from poor injection of cells. DOX treatment was started at two different time points. 1) Two days following cell inoculation, mice were separated into DOX-treated (+DOX Day 2) and control no DOX group. DOX was provided as 2mg/ml with water supplemented with sucrose. Tumor dimensions were recorded three times per week with a digital caliper and the tumor volume was estimated as $V\ (mm^3) = \pi/6(\text{length} \times \text{width}^2)$. When tumors reached 50–70 mm^3 mice were randomized and segregated into DOX-treated (+DOX Day 9) and control no DOX group. Results were analyzed for statistical significance using two-tailed Student's *t*-test with GraphPad software.

Supplementary Material

Refer to Web version on PubMed Central for supplementary material.

Acknowledgements

The authors wish to thank Drs. Andrei Karginov, Todd Waldman, Gregory Thatcher, Bernard Weisman and Robert Winn for providing various cell lines. In addition, we wish to thank Drs. Shohei Koide and Andrei Karginov along with the O'Bryan and Karginov labs for many helpful discussions. R.S.S was supported by an NIH F31 Predoctoral Award (CA192822). This work was supported in part by a Merit Review Award (1I01BX002095) from the United States (U.S.) Department of Veterans Affairs Biomedical Laboratory Research and Development Service and NIH awards (CA212608 and CA201717) to J.P.O. The contents of this article do not represent the views of the U.S. Department of Veterans Affairs or the United States Government.

References:

1. Spencer-Smith R, O'Bryan JP. Direct inhibition of RAS: Quest for the Holy Grail? Semin Cancer Biol 2017 12 14;
2. Karnoub AE, Weinberg RA. Ras oncogenes: split personalities. Nat Rev Mol Cell Biol 2008 7;9(7): 517–31. [PubMed: 18568040]
3. Cox AD, Der CJ. Ras history: The saga continues. Small GTPases 2010 7;1(1):2–27. [PubMed: 21686117]
4. Vigil D, Cherfils J, Rossman KL, Der CJ. Ras superfamily GEFs and GAPs: validated and tractable targets for cancer therapy? Nat Rev Cancer 2010 12;10(12):842–57. [PubMed: 21102635]
5. Cherfils J, Zeghouf M. Regulation of small GTPases by GEFs, GAPs, and GDIs. Physiol Rev 2013 1;93(1):269–309. [PubMed: 23303910]
6. Simanshu DK, Nissley DV, McCormick F. RAS Proteins and Their Regulators in Human Disease. Cell 2017 6 29;170(1):17–33. [PubMed: 28666118]
7. Cox AD, Fesik SW, Kimmelman AC, Luo J, Der CJ. Drugging the undruggable RAS: Mission possible? Nat Rev Drug Discov 2014 11;13(11):828–51. [PubMed: 25323927]
8. Lerner EC, Qian Y, Hamilton AD, Sebti SM. Disruption of oncogenic K-Ras4B processing and signaling by a potent geranylgeranyltransferase I inhibitor. J Biol Chem 1995 11 10;270(45):26770–3. [PubMed: 7592913]
9. Whyte DB, Kirschmeier P, Hockenberry TN, Nunez-Oliva I, James L, Catino JJ, et al. K- and N-Ras are geranylgeranylated in cells treated with farnesyl protein transferase inhibitors. J Biol Chem 1997 5 30;272(22):14459–64. [PubMed: 9162087]

Author Manuscript Author Manuscript Author Manuscript Author Manuscript

10. Güldenhaupt J, Rudack T, Bachler P, Mann D, Triola G, Waldmann H, et al. N-Ras forms dimers at POPC membranes. Biophys J 2012 10 3;103(7):1585–93. [PubMed: 23062351]
11. Lin W-C, Iversen L, Tu H-L, Rhodes C, Christensen SM, Iwig JS, et al. H-Ras forms dimers on membrane surfaces via a protein-protein interface. Proc Natl Acad Sci U S A 2014 2 25;111(8): 2996–3001. [PubMed: 24516166]
12. Nan X, Tamgüney TM, Collisson EA, Lin L-J, Pitt C, Galeas J, et al. Ras-GTP dimers activate the Mitogen-Activated Protein Kinase (MAPK) pathway. Proc Natl Acad Sci U S A 2015 6 30;112(26):7996–8001. [PubMed: 26080442]
13. Plowman SJ, Muncke C, Parton RG, Hancock JF. H-ras, K-ras, and inner plasma membrane raft proteins operate in nanoclusters with differential dependence on the actin cytoskeleton. Proc Natl Acad Sci U S A 2005 10 25;102(43):15500–5. [PubMed: 16223883]
14. Kovrigina EA, Galiakhmetov AR, Kovrigin EL. The Ras G Domain Lacks the Intrinsic Propensity to Form Dimers. Biophys J 2015 9 1;109(5):1000–8. [PubMed: 26331257]
15. Chung JK, Lee YK, Denson J-P, Gillette WK, Alvarez S, Stephen AG, et al. K-Ras4B Remains Monomeric on Membranes over a Wide Range of Surface Densities and Lipid Compositions. Biophys J 2018 1 9;114(1):137–45. [PubMed: 29320680]
16. Santos E Dimerization Opens New Avenues into Ras Signaling Research. Sci Signal 2014 5 6;7(324):pe12–pe12. [PubMed: 24803535]
17. Spencer-Smith R, Koide A, Zhou Y, Eguchi RR, Sha F, Gajwani P, et al. Inhibition of RAS function through targeting an allosteric regulatory site. Nat Chem Biol 2017 1;13(1):62–8. [PubMed: 27820802]
18. Spencer-Smith R, Li L, Prasad S, Koide A, Koide S, O'Bryan JP. Targeting the α4-α5 interface of RAS results in multiple levels of inhibition. Small GTPases 2017 7 10;1–10.
19. Kim J-S, Lee C, Foxworth A, Waldman T. B-Raf is dispensable for K-Ras-mediated oncogenesis in human cancer cells. Cancer Res 2004 3 15;64(6):1932–7. [PubMed: 15026326]
20. Vartanian S, Bentley C, Brauer MJ, Li L, Shirasawa S, Sasazuki T, et al. Identification of mutant K-Ras-dependent phenotypes using a panel of isogenic cell lines. J Biol Chem 2013 1 25;288(4): 2403–13. [PubMed: 23188824]
21. Porter AG, Jänicke RU. Emerging roles of caspase-3 in apoptosis. Cell Death Differ 1999 2;6(2): 99–104. [PubMed: 10200555]
22. Ostrem JM, Peters U, Sos ML, Wells JA, Shokat KM. K-Ras(G12C) inhibitors allosterically control GTP affinity and effector interactions. Nature 2013 11 28;503(7477):548–51. [PubMed: 24256730]
23. Janes MR, Zhang J, Li L-S, Hansen R, Peters U, Guo X, et al. Targeting KRAS Mutant Cancers with a Covalent G12C-Specific Inhibitor. Cell 2018 1 25;172(3):578–589.e17. [PubMed: 29373830]
24. Muzumdar MD, Chen P-Y, Dorans KJ, Chung KM, Bhutkar A, Hong E, et al. Survival of pancreatic cancer cells lacking KRAS function. Nat Commun 2017 23;8(1):1090. [PubMed: 29061961]
25. Ambrogio C, Köhler J, Zhou Z-W, Wang H, Paranal R, Li J, et al. KRAS Dimerization Impacts MEK Inhibitor Sensitivity and Oncogenic Activity of Mutant KRAS. Cell 2018 2 8;172(4):857–868.e15. [PubMed: 29336889]
26. Clark GJ, Cox AD, Graham SM, Der CJ. Biological assays for Ras transformation. Methods Enzymol 1995;255:395–412. [PubMed: 8524126]

Author Manuscript Author Manuscript Author Manuscript Author Manuscript

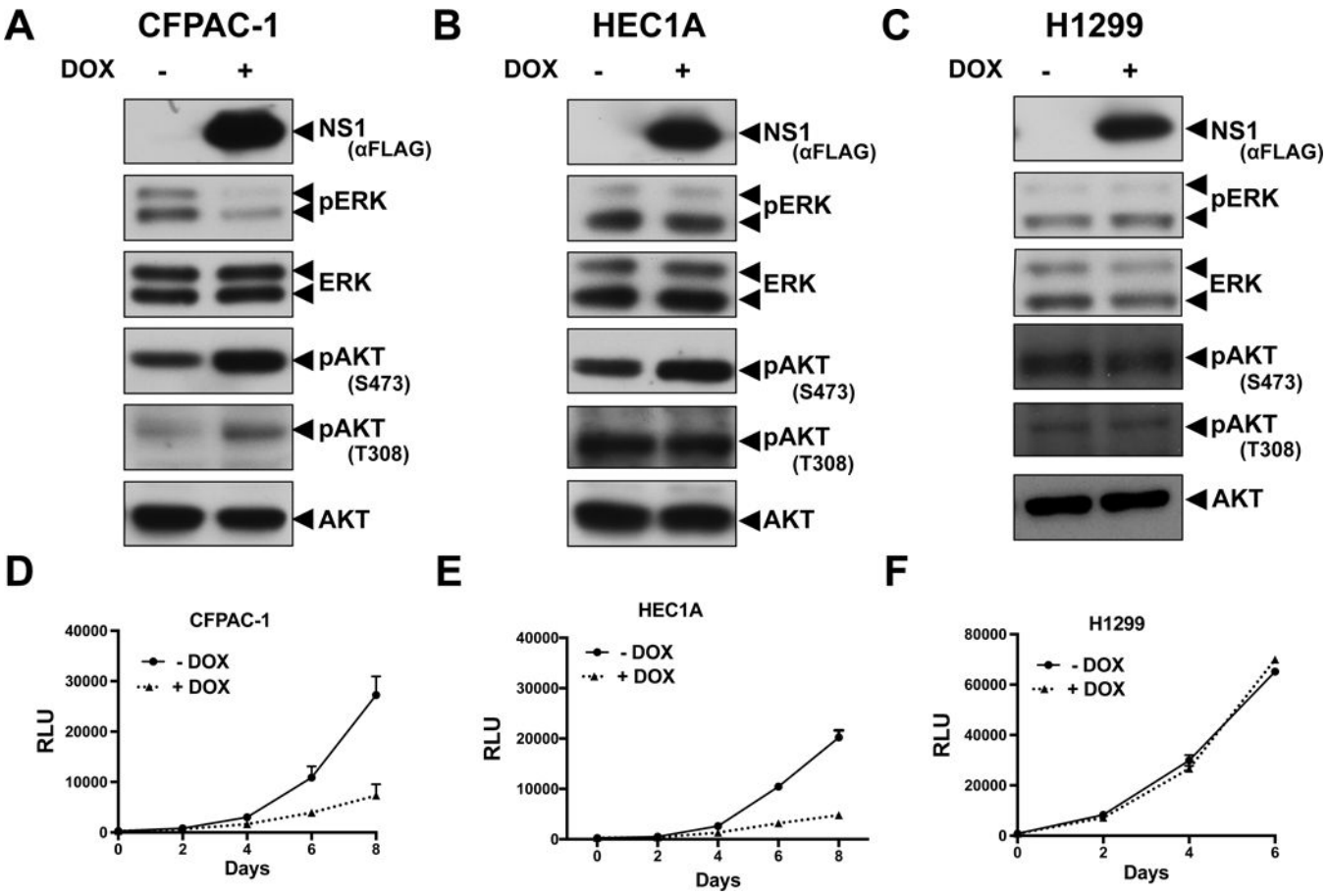

Figure 1. Targeting the α4-α5 interface impairs signaling and cell proliferation in K-RAS mutant tumor cells.

Doxycycline (DOX) inducible NS1 expressing stable lines were generated from K-RAS and N-RAS mutant tumor cells. (**A**) Western blot analysis of CFPAC-1 cells [K-RAS(G12V)] +/− DOX treatment. ERK and AKT activation was measured using phosphospecific antibodies. (**B**) Western blot analysis of HEC1A cells [K-RAS(G12D)] +/− DOX. ERK and AKT activation were measured as in A. **(C)** Western blot analysis of H1299 cells [N-RAS(Q61K)] +/− DOX. ERK and AKT activation were measured as in A. (**D–F**) Proliferation was measured in the indicated tumor cell lines +/− (DOX) using Promega Cell TiterGlo luciferase assay. Results represent the average +/− *s.d.* of two experiments each performed with triplicate wells.

Author Manuscript Author Manuscript Author Manuscript Author Manuscript

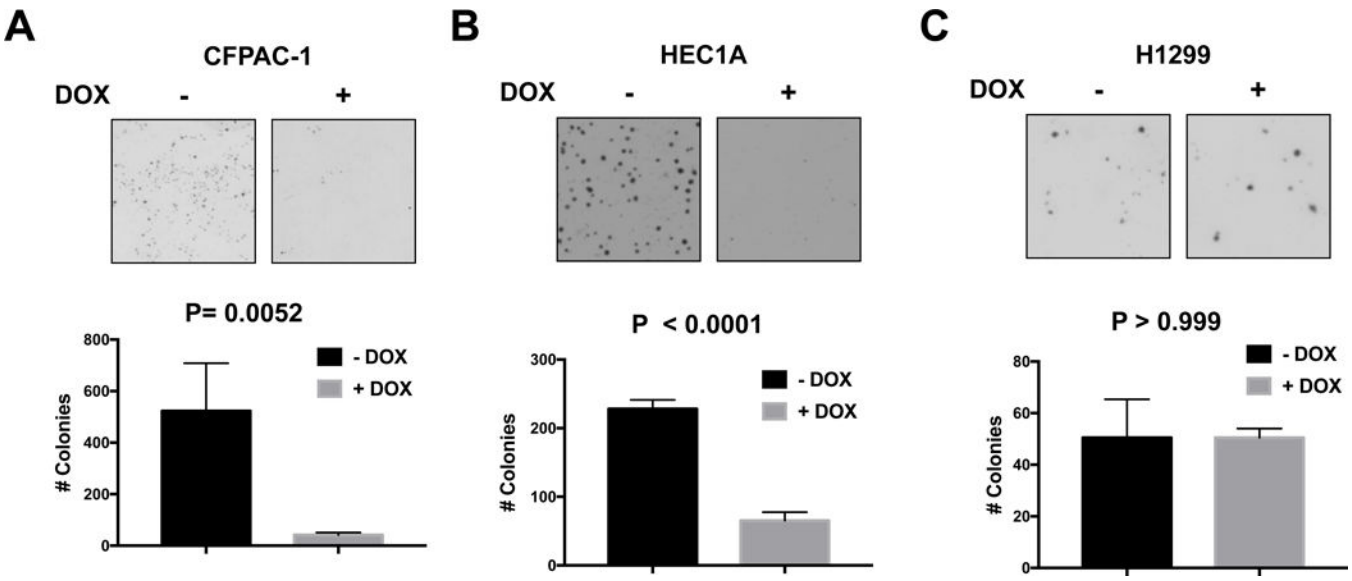

Figure 2. Targeting the α4-α5 interface reduces anchorage-independent growth of K-RAS mutant tumor cells.

Various K-RAS and N-RAS mutant lines were plated in soft agar and then treated with (+) or without (–) DOX. Media was replenished every two days and colony formation was analyzed after 21days. The graphs show the average colony number per well from 3 wells ± *s.d.*. Colonies were counted using NIH ImageJ software. Images are representative wells from each assay. (**A**) CFPAC-1 pancreatic tumor cells; (**B**) HEC1A, endometrial tumor cells; (**C**) H1299, lung cancer line.

Author Manuscript Author Manuscript Author Manuscript Author Manuscript

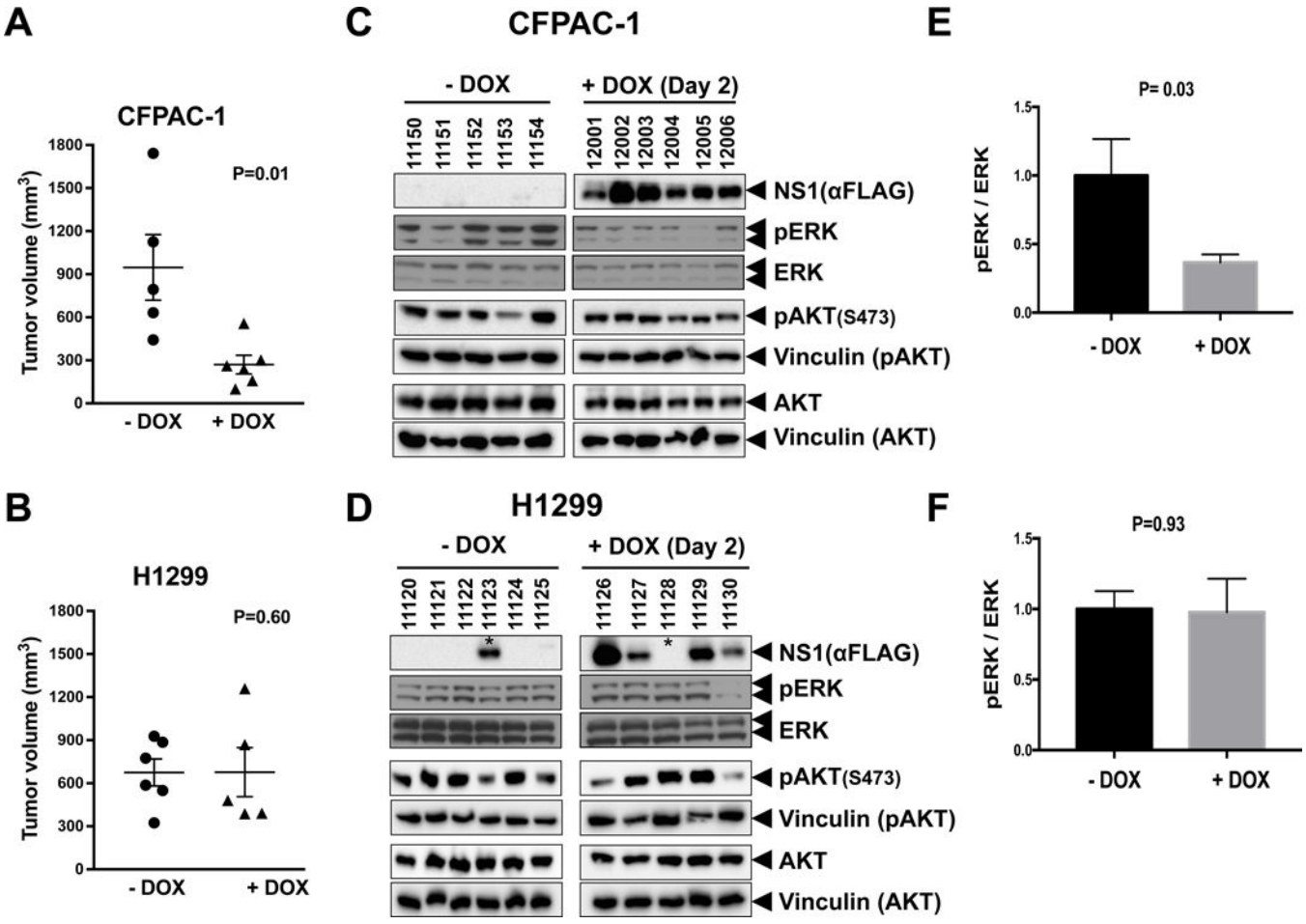

Figure 3. NS1-mediated inhibition of RAS reduces K-RAS driven tumor formation.

(A&B) Xenograft assays were performed with CFPAC-1 cells **(A)** and H1299 cells **(B).** Two days after s.c. injection of tumor cells, mice were separated into control group (-DOX; n= 5 for CFPAC-1, n=6 for H1299) or DOX-treated (+DOX; n= 6 for CFPAC1 n= 5 for H1299). Average tumor volume is shown as a horizontal line with the *s.e.m.* noted by the bar. Volume of each tumor is indicated in the graph. P values were calculated using a two tailed Student's *t*-test. **(C&D)** Western blot analysis of cell signaling in tumor cell lysates was performed as in Fig. 1. The asterisks in **(D)** denote samples that appear to have been switched between treated and control groups. **(E&F)** Quantification of pERK activation in tumor lysates from **(C&D)** was done using NIH Image as previously described(17) and presented as relative pERK activation compared to untreated samples. Error bars represent *s.e.m.* P values are indicated above the graphs and were calculated using a Student's *t*-test.

Author Manuscript Author Manuscript Author Manuscript Author Manuscript

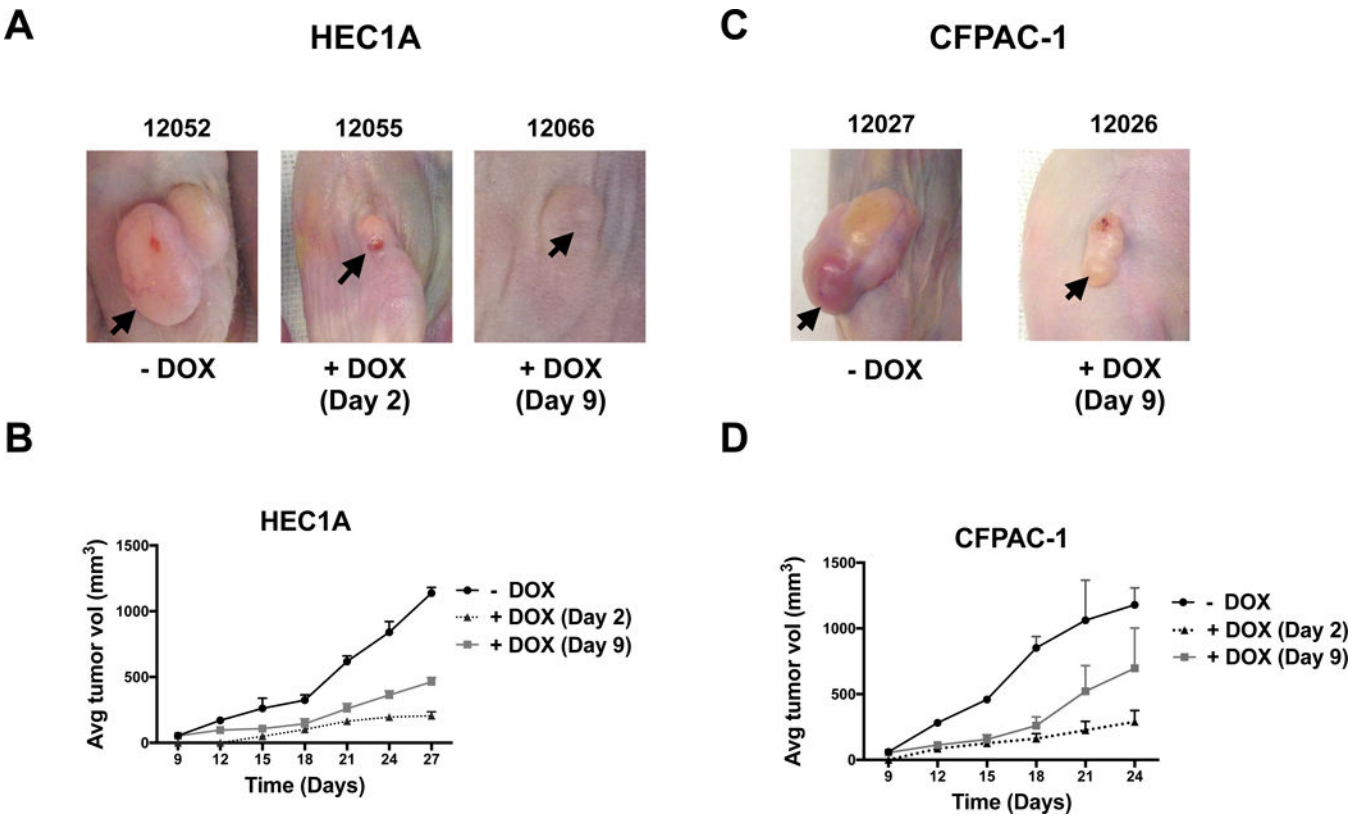

Figure 4. Targeting the α4-α5 interface decreases K-RAS driven tumor development and progression.

(**A**) HEC1A cells were injected into female athymic nude mice and then separated into three groups: 1) no DOX treatment (-DOX); 2) DOX treatment beginning 2 days after injection, +DOX (Day 2); 3) DOX treatment upon tumor reaching 50–70 mm^3, +DOX (Day 9). N=4 for each condition. Arrows denote tumors in mice upon sacrifice of animals. (**B**) Tumor kinetics of HEC1A cells. Tumor dimensions were recorded 3 times a week using a digital caliper. Data are presented as mean tumor volume ± *s.d.* (**C**) Same as **(A)** except CFPAC-1 cells were injected into athymic nude mice. N=6 for each condition (3 male and 3 female). **(D)** Tumor kinetics of CFPAC-1 cells were measured as in **(B)**. Data are presented as mean tumor volume ± *s.d.*

Author Manuscript Author Manuscript Author Manuscript Author Manuscript

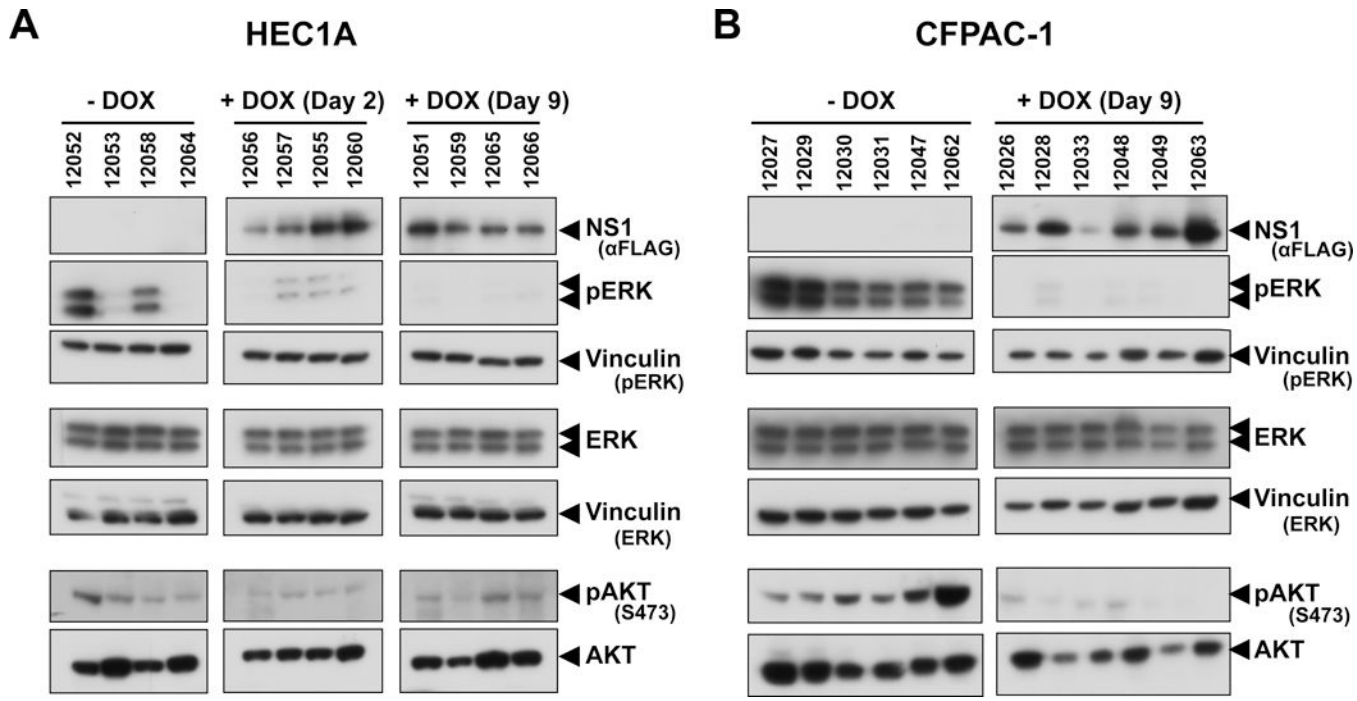

Figure 5. NS1 inhibition of RAS blocks oncogenic K-RAS signaling *in vivo*.

Lysates of HEC1A (A) and CFPAC-1 (B) tumors were analyzed by Western blot for activation of ERK and AKT as in Fig. 1. NS1 expression was only observed in DOX treated mice. Vinculin was used as a normalization control for ERK and pERK blots.

Author Manuscript Author Manuscript Author Manuscript Author Manuscript

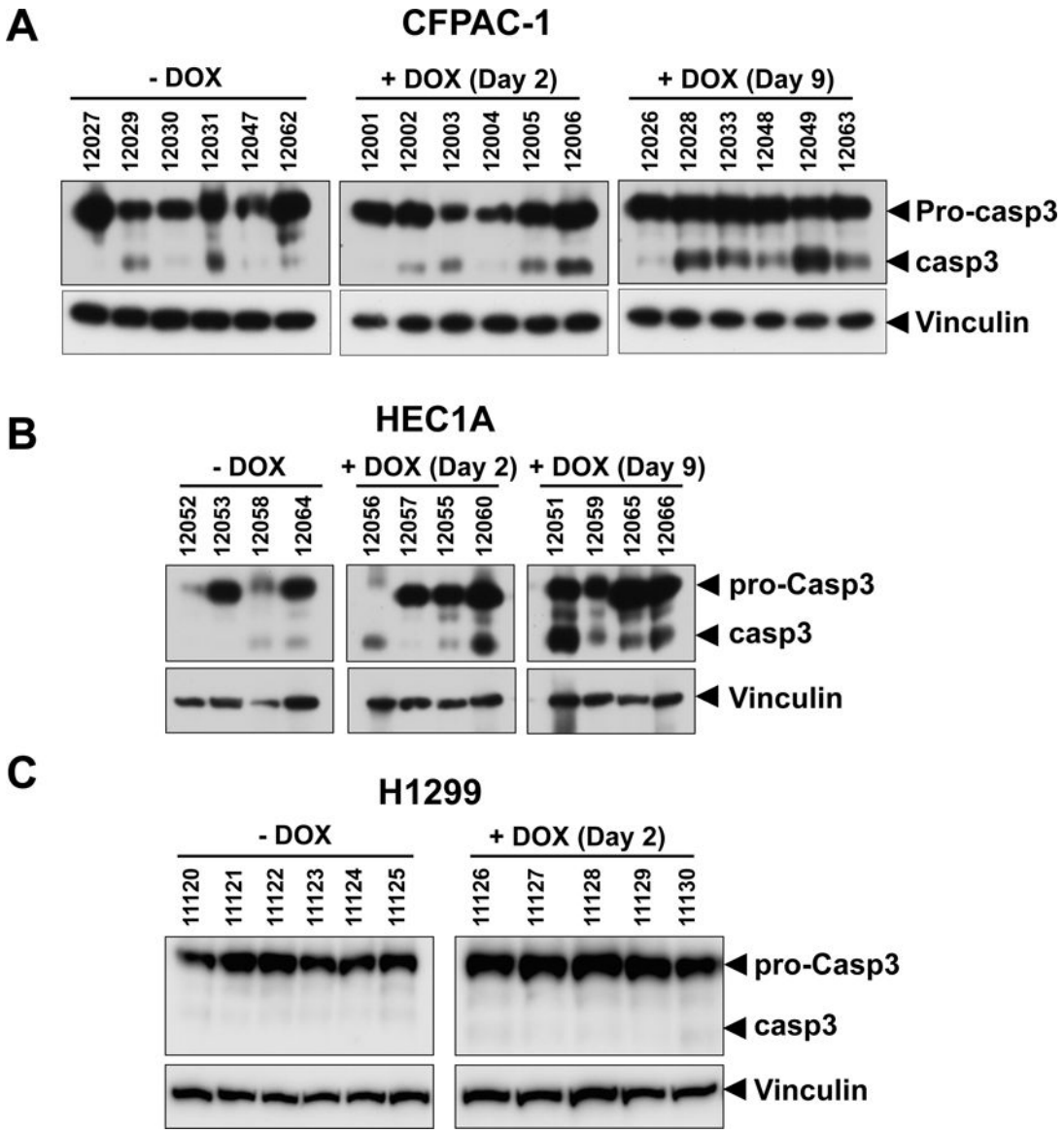

Figure 6. NS1 targeting of the α4-α5 interface induces apoptosis in K-RAS but not N-RAS mutant tumors.

Apoptosis was analyzed by measuring proteolytic cleavage of caspase-3 by Western blot analysis of tumor lysates. **(A)** CFPAC-1 tumor lysates. **(B)** HEC1A tumor lystes **(C)** H1299 tumor lysates. Vinculin was used as a normalization control for loading. Pro-casp3, pro-caspase3; casp3, mature, proteolytically activated caspase3.